

# Detailed Theoretical Investigations on the L-Shell Absorption of Open-M-Shell Germanium Plasmas: Effect of Autoionization Resonance Broadening

Wenjun Xiang, Jiaolong Zeng, Yongsheng Fu, Cheng Gao

Department of Physics, College of Science, National University of Defense Technology, Changsha, China

Email: xiangwenjun89@163.com

Received August 23, 2012; revised September 25, 2012; accepted October 2, 2012

## ABSTRACT

Radiative opacity of open-M-shell germanium plasmas in the L-shell photon energy region were investigated in detail by using a fully relativistic detailed level accounting approach. Among other physical effects such as relativistic and the interaction between fine-structure levels belonging to the same non-relativistic configuration and different configurations, particular attention is paid on the effect of autoionization resonance broadening on the L-shell absorption. The results show that for plasmas at present and past typical experimental conditions, line width due to autoionization resonance broadening dominate among all the physical broadening mechanisms including electron impact and Doppler broadenings. Such an effect is most pronounced for ions with just a few 2p-nd transition lines such as  $Ge^{14+}$ , while it is not so pronounced for complex ions such as  $Ge^{16+}$ , where there are so many 2p-nd lines that line overlapping partly conceal the effect of autoionization resonance broadening. After taking the effect of autoionization resonance broadening into account, detailed comparisons are made with available experimental spectra at different physical conditions of different plasma temperatures and densities. The L-shell absorption is sensitive to the plasma temperature, especially in the 2p-3d excitation energy region. The potential of utilizing the relative shape and intensity of the 2p-3d spin-orbit splitting as temperature diagnostics is investigated.

**Keywords:** Autoionization Resonance Broadening; Germanium; Absorption; Radiative Opacity

## 1. Introduction

Germanium is one of the absorption and switching material in indirectly driven inertial confinement fusion and therefore its radiative property is of great interest both experimentally and theoretically [1-9]. The radiative opacity of open-M-shell germanium plasmas are of particular experimental interest, especially in the region of 2p-3d and 2p-4d transition arrays. Foster *et al.* [1] measured the L-shell absorption spectrum of a germanium plasma, which was generated by radiation heating using thermal X radiation from a laser-produced gold plasma. Tracer elements of Al and Mg were used to characterize the temperature (76 eV) and density ( $0.05 \text{ g/cm}^3$ ) of the plasma. Perry *et al.* [2] experimentally measured the X-ray absorption of germanium plasmas at a lower temperature of about 38 eV. Renaudin *et al.* [3] measured the absorption spectra of germanium plasma in the 0.8 - 1.1 nm range. The germanium sample was radiatively heated by a gold hohlraum. Recently, Loisel *et al.* [4] experimentally measured the radiative opacity of medium Z element plasmas including germanium in the X-ray re-

gion (0.8 - 1.8 nm) at temperatures between 15 and 25 eV and densities between 2 and  $10 \text{ mg/cm}^3$ .

The experimental observations provide valuable data to validate different approximations made in the opacity calculations. In order to interpret these experiments, various theoretical methods were used to analyze the observed spectra. Foster *et al.* [1] used a detailed configuration accounting (DCA) model which includes an approximate treatment of term widths using the unresolved transition array (UTA) approach. Perry *et al.* [2] employed a Super Transition Array (STA) approach [10] to describe the state of plasmas, which can be thought as a hybrid approach between an average atom description and a full DCA scheme. In these statistical methods, the line width caused by the statistical approach are generally dominant and therefore a Gaussian line shape is used. Renaudin *et al.* [3] took into account of the term structure using UTA statistical methods and a detailed line accounting approach in pure jj coupling with orbital relaxation effect being considered. In their work, a Gaussian shape is used, which assumed that Doppler broadening

dominates all other broadening mechanisms.

In a recent work, Blenski *et al.* [11] carried out theoretical interpretation of the X-ray photo-absorption experiments measured at LULI2000 facility [4]. Their analysis was performed using the statistical superconfiguration code SCO, two line-by-line opacity codes based on the HULLAC and FAC packages and a hybrid statistical-detailed code SCORCG. The authors pointed out that in the detailed line-by-line treatment the autoionization (AI) resonance broadening appeared to be the most important in all broadening mechanisms. Yet no detailed investigations were found in the literature on this effect partly due to the very challenging computations of the detailed line spectrum with the complex open-M-shell Ge ions.

With the development of computational ability, computation of plasma opacities is developing toward more accurate direction including DLA, mixed DLA and UTA and improvement of UTA [12-14]. In this work, we investigated the radiative opacity of Ge plasmas by using a detailed level accounting (DLA) approach. In such a DLA method, we do not need to introduce additional line broadening caused by the statistical method, and therefore we include only true physical broadening mechanisms such as Doppler, electron impact and AI resonance broadenings. Among other physical effects on the opacity, particular attention was paid on the effect of AI resonance broadening of L-shell excitation region. To the best of our knowledge, no detailed systematic investigations were found in the literature on this physical effect on the L-shell absorption of open-M-shell germanium plasmas, although many researches (for example, see [15-21]) highlighted the importance of AI process to determine the population balance and radiative properties in non-local thermodynamic equilibrium (non-LTE) plasmas with a wide range of temperature and density.

## 2. Theoretical Method

The total radiative opacity for a plasma at a temperature  $T$  and mass density  $\rho$  is the sum of the bound-bound, bound-free, free-free and scattering processes. The contribution of bound-bound process for radiation of energy  $h\nu$  can be obtained from the cross sections of bound-bound lines:

$$\rho\kappa_{bb} = \sum_i \left[ \sum_{l'} N_{il} \sigma_{ll'}(h\nu) \right] \quad (1)$$

where  $N_{il}$  is the population density of level  $l$  of ionization stage  $i$  and  $\sigma_{ll'}(h\nu)$  is the cross section for photoexcitation from level  $l$  to  $l'$  of ionization state  $i$  and can be expressed in terms of the absorption oscillator strength  $f_{ll'}$  as

$$i\sigma_{ll'}(h\nu) = \frac{\pi h e^2}{mc} f_{ll'} S(h\nu) \quad (2)$$

where  $h$  is the Planck constant,  $c$  is the speed of light in vacuum,  $e$  is the electron charge,  $m_e$  is the rest mass of electron, and  $S(h\nu)$  is the line shape function. In the DLA approach, the line shape function takes the Voigt profile:

$$S(h\nu) = \frac{\sqrt{\ln 2}}{\sqrt{\pi}\Gamma_d} H(a, \nu) \quad (3)$$

where  $H(a, \nu)$  is the Voigt function:

$$H(a, \nu) = \frac{a}{\pi} \int_{-\infty}^{+\infty} \frac{e^{-x^2}}{a^2 + (\nu - x)^2} dx$$

$$a = \sqrt{\ln 2} \Gamma_l / \Gamma_d$$

$$\nu = \sqrt{\ln 2} (h\nu - h\nu_0) / \Gamma_d$$

where  $\Gamma_d$  and  $\Gamma_l$  are the Doppler and Lorentzian half width at half maximum (HWHM), respectively. The Doppler HWHM is related to the temperature  $T$  of the plasma and transition energy  $h\nu_0$  [22]:

$$\Gamma_d = 3.858 \times 10^{-5} (kT/A)^{1/2} (h\nu_0) \quad (4)$$

where  $A$  is atomic weight of the ion in gram and the units of  $kT$ ,  $h\nu_0$  and  $\Gamma_d$  are eV. The Lorentzian HWHM ( $\Gamma_l$ ) is contributed by the electron impact broadening ( $\Gamma_e$ ), AI resonance broadening ( $\Gamma_a$ ) and natural life broadening. In general, line width due to natural life are much smaller than the electron impact and AI resonance broadening. Yet the line width caused by AI resonance broadening is in many cases the dominant broadening mechanism and therefore should be taken into account. The accurate determination of the AI resonance broadening is complicated because of the complex atomic structure for open-M-shell Ge ions and thus is not carefully considered in previous work. In this work, we systematically investigated the effect of AI resonance broadening on the L-shell absorption of open-M-shell Ge plasmas. For the line width of electron impact broadening, we use a semiempirical method [23,24]

$$\Gamma_e = N_e \frac{8\pi}{6} \frac{\hbar^3}{m^2 e} \left( \frac{2m}{\pi kT} \right)^{1/2} \frac{\pi}{\sqrt{3}} \left( 0.9 - \frac{1.1}{z} \right)$$

$$\sum_{j=i,f} \left( \frac{3n_j}{2z} \right)^2 (n_j^2 - l_j^2 - l_j - 1) \quad (5)$$

where  $n_i^2$  ( $l_i$ ) and  $n_f^2$  ( $l_f$ ) are the effective principal (orbital angular momentum) quantum numbers of the lower and upper energy levels of the transition, respectively.

The contribution of bound-free opacity  $\kappa_{bf}$  can be

obtained from the photoionization cross sections per ion:

$$\rho\kappa_{bf} = \sum_{i,l} N_{il} \sigma_{il}(h\nu) \quad (6)$$

where  $N_{il}$  is the total population density of all possible levels of ionization stage  $i$  and  $\sigma_i(h\nu)$  is the photoionization cross section per ion  $i$  and it can be calculated from the photoionization cross sections  $\sigma_{il}(h\nu)$  from level  $l$  in ion  $i$

$$\sigma_i(h\nu) = \sum_l \frac{g_{il} e^{-E_{il}/kT}}{Z_i} \sigma_{il}(h\nu) \quad (7)$$

where  $g_{il}$  is the statistical weight for level  $l$  of ion  $i$ ,  $E_{il}$  is the energy of level  $l$  of ion  $i$  above the ground state and  $Z_i$  is the partition function for ion  $i$ .

In the X-ray region, the bound-bound and bound-free contributions to the opacity are generally dominant and thus only simple approximations are used to describe the free-free (Kramers cross section) and scattering (Thompson scattering cross section) contribution to the opacity.

The population density of different charge states  $N_i$  is determined by ionization equilibrium equation in LTE. For a particular level of each charge state, the population density obeys the Boltzmann distribution. The ionization potential depression is considered by using the Debye-Huckel model [25].

The fraction of radiation transmitted with respect to some incident source of arbitrary intensity is given by

$$F(h\nu) = e^{-\rho\kappa(h\nu)L} \quad (8)$$

where  $L$  is the path length traversed by the light source through the plasma. To compare directly with experiment, one should include the effects of instrumental broadening.

### 3. Results and Discussion

For the experimental conditions [1-4], the charge states which contribute to the L-shell absorption range from  $Ge^{5+}$  (the ground configuration  $[Ne]3s^23p^63d^9$ ) to  $Ge^{21+}$  (the ground configuration  $[Ne]3s$ ). For these ionization stages of Ge, the upper levels of 2p-nd transitions are autoionized ones, and therefore it is necessary to include the effect of AI resonance broadening on the L-shell absorption. These charge states have complex atomic structure with an open-M-shell characteristics and it is a challenging work to accurately determine the atomic data including energy levels, oscillator strengths, photoionization cross sections and line width due to autoionized levels.

In order to take into account of the configuration interaction (CI), an atomic state is approximated by a linear combination of configuration state functions (CSFs) with same symmetry

$$\Phi_\alpha(J\pi) = \sum_i^{n_c} a_i(\alpha) \phi_\alpha(J\pi) \quad (9)$$

where  $n_c$  is the number of CSFs and  $a_i(\alpha)$  denotes the representation of the atomic state in this basis. The CSFs are anti-symmetrized products of a common set of orthogonal orbitals which are optimized on the basis of the relativistic Hamiltonian. Once the CI wavefunctions have been obtained, the oscillator strengths can be calculated

$$g_i f_{ij} = \frac{2\Delta E}{3} \left| \langle \Phi_i | \mathbf{P} | \Phi_j \rangle \right|^2 \quad (10)$$

where  $\Delta E = E_j - E_i$ ,  $E_i$  and  $E_j$  are, respectively, the energies of initial and final levels and  $g_i$  is the statistical weight of the lower state, *i.e.*  $g_i = 2J_i + 1$ .  $\mathbf{P}$  is dipole transition operator with  $\mathbf{P} = \sum_{p=1}^N \mathbf{r}_p$  in the length

formalism and  $\mathbf{P} = \frac{2}{\Delta E} \sum_{p=1}^N \nabla_p$  in the velocity formalism,

where  $N$  is the total number of bound electrons. The AI rates are obtained in the relativistic distorted-wave approximation, which reads in the first order perturbation theory (in atomic units)

$$A_{ij}^a = 2 \sum_{\kappa} \left| \left\langle \psi_j, \kappa; J_T M_T \left| \sum_{i < j} \frac{1}{r_{ij}} \right| \psi_i \right\rangle \right|^2 \quad (11)$$

where  $\psi_i$  is the autoionizing state,  $\psi_f$  is the final state which has one less electron than  $\psi_i$ ,  $\kappa$  is the relativistic angular quantum number of the free electron. The total angular quantum number of the coupled final state must be equal to that of  $\psi_i$ , *i.e.*,  $J_T = J_i$  and  $M_T = M_i$ . The AI resonance width of level  $i$  can be obtained by summing all final levels

$$\Gamma_i^a = \hbar \sum_j A_{ij}^a \quad (12)$$

where  $\hbar = h/2\pi$ . All atomic data required in the calculation of opacity were obtained out using the Flexible Atomic Code (FAC) developed by Gu [26].

We first investigate the effect of AI resonance broadening on the opacity of Ge plasma. Extensive calculations were carried out and the results show that the AI resonance HWHM for the inner shell 2p excited levels range from 0.05 eV to 0.4 eV for charge states from  $Ge^{5+}$  to  $Ge^{20+}$ . For  $Ge^{14+}$ , the ground configuration  $[Ne]3s^23p^6$  only has one fine-structure level. The 2p excited configuration  $2p^53s^23p^63d$  is split into 12 fine-structure levels, where  $(2p_{3/2}^{-1}3d_{3/2})_1$ ,  $(2p_{3/2}^{-1}3d_{5/2})_1$ , and  $(2p_{1/2}^{-1}3d_{3/2})_1$  the total angular momentum is 1.  $(2p_{3/2}^{-1}3d_{3/2})_1$  means one hole in orbital 2p, one electron in orbital 3d and full electron orbitals have been omitted.

For the 2p-3d transition array, there are three dipole allowed transitions:  $2p_{3/2} - 3d_{3/2}$ ,  $2p_{3/2} - 3d_{5/2}$ , and  $2p_{1/2} - 3d_{3/2}$ . The radiative transition probability of the first transition is much smaller than the last two lines. The effect of AI resonance width on the absorption in the 2p-3d region can clearly be seen from **Figure 1**, which shows the absorption cross section for the transition array of  $2p^6 3s^2 3p^6 - 2p^5 3s^2 3p^6 3d$  of  $Ge^{14+}$ . In order to obtain the results,  $Ge^{14+}$  was assumed to be embedded in an LTE plasma at a temperature of 60 eV and a density of 0.01 g/cm<sup>3</sup>. In **Figure 1(b)**, the electron impact broadening and Doppler broadening mechanisms are considered, while the AI resonance broadening is not included. In **Figure 1(a)**, three broadening mechanisms are all taken into account. One can see that when AI resonance broadening is included, the peak absorption cross section is one order of magnitude smaller, which is a reflection of the effect of AI resonance broadening on the absorption. In the above plasma condition, the HWHM due to electron impact and Doppler broadening is evaluated to be 0.003 eV and 0.041 eV, respectively. The HWHM due to AI resonance broadening is calculated to be 0.247 eV and 0.263 eV for 2p excited levels of  $(2p_{3/2}^{-1} 3d_{5/2})_1$  and  $(2p_{1/2}^{-1} 3d_{3/2})_1$ , respectively. Among the three broadening mechanisms, the AI resonance broadening is the dominant broadening mechanism. The AI resonance width is larger than the electron impact and Doppler width by more than one order of magnitude.

The effect of AI resonance broadening on the absorption of  $Ge^{14+}$  is evident from the inspection of **Figure 1**. As there are only two strong absorption lines and the 2p-3d spin-orbit splitting ( $\sim 30$  eV) is much larger than

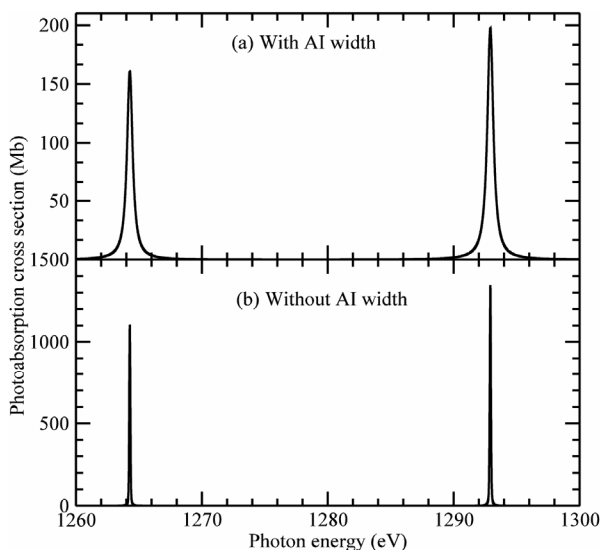


**Figure 1.** Absorption cross section for the transition array  $2p^6 3s^2 3p^6 - 2p^5 3s^2 3p^6 3d$  of  $Ge^{14+}$ : (a) including and (b) not including the effect of AI resonance broadening.

the line width caused by all broadening mechanisms, two 2p-3d transition lines are separate each other with an interval of  $\sim 30$  eV. With the decrease of the number of 3p electrons, especially near the half full 3p orbital, the number of 2p-3d lines becomes rapidly great and the absorption approaches unresolved quasi-continuum bands. **Figure 2** shows the absorption cross section for the transition array of  $2p^6 3s^2 3p^4 - 2p^5 3s^2 3p^4 3d$  of  $Ge^{16+}$ , which was assumed to be embedded in an LTE plasma at a temperature of 90 eV and a density of 0.015 g/cm<sup>3</sup>. Similar to  $Ge^{14+}$ , the AI resonance width is also larger than the electron impact and Doppler width by more than one order of magnitude. Yet the peak absorption cross section without considering the AI resonance broadening is just 2.43 times larger than that which includes this effect. This is due to many lines overlapped together resulting in less pronounced for the effect of AI resonance broadening than in  $Ge^{14+}$ , where lines do not overlap. The two strong absorption bands with an interval of spin-orbit splitting of  $\sim 30$  eV in **Figure 2** originate from  $2p_{3/2} - 3d_{5/2}$  and  $2p_{1/2} - 3d_{3/2}$  transitions for the lower and higher photon energy range, respectively. Such a feature differ obviously from that of  $Ge^{14+}$ . With the further decrease of ionization stage, the 2p-3d absorption shows a different feature from  $Ge^{14+}$  and  $Ge^{16+}$ , as illustrated in **Figure 3**, which shows the absorption cross section for the transition array of  $2p^6 3s^2 3p^6 3d^5 - 2p^5 3s^2 3p^6 3d^6$  of  $Ge^{9+}$ .  $Ge^{9+}$  was assumed to be embedded in an LTE plasma at a temperature of 38 eV and a density of 0.015 g/cm<sup>3</sup>. For  $Ge^{14+}$  and  $Ge^{16+}$ ,  $2p_{3/2} - 3d_{5/2}$  absorption is weaker than  $2p_{1/2} - 3d_{3/2}$ , while this is reversed for  $Ge^{9+}$ . Fur-

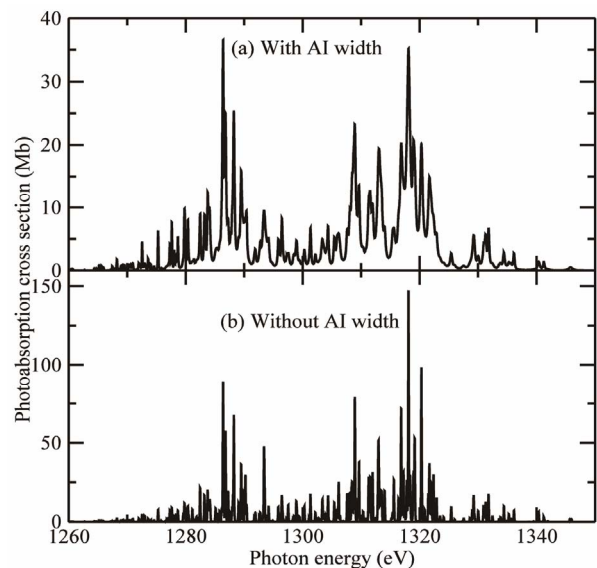


**Figure 2.** Absorption cross section for the transition array  $2p^6 3s^2 3p^4 - 2p^5 3s^2 3p^4 3d$  of  $Ge^{16+}$ : (a) including and (b) not including the effect of AI resonance broadening.

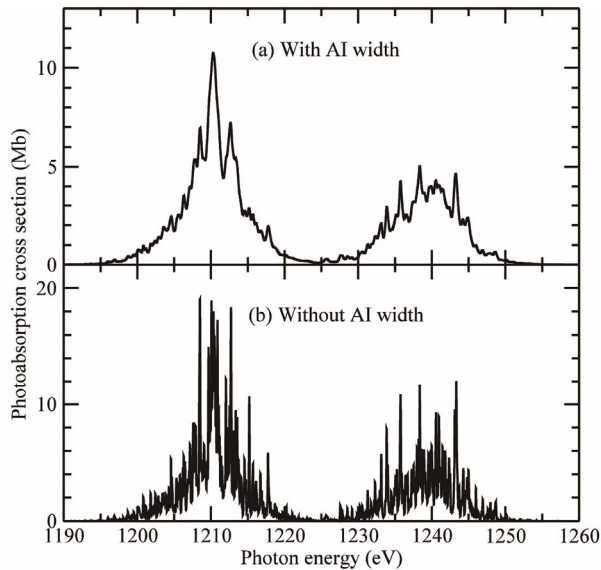


**Figure 3.** Absorption cross section for the transition array  $2p^6 3s^2 3p^6 3d^5 - 2p^5 3s^2 3p^6 3d^6$  of  $\text{Ge}^{9+}$ : (a) including and (b) not including the effect of AI resonance broadening.

thermore, the AI width for many upper levels of  $2p_{3/2} - 3d_{5/2}$  transitions is much smaller than those of  $2p_{1/2} - 3d_{3/2}$ .

As an illustrative example, **Figure 4** shows the effect of AI resonance broadening on the radiative opacity of Ge plasma at a temperature of 38 eV and a density of  $0.015 \text{ g/cm}^3$  with plot (a) including and (b) not including such an effect. Due to many overlapped lines, it was found that the effect of AI resonance broadening reduce the peak value of opacity by only 25% for 2p-3d transition arrays. For 2p-4d and higher transition arrays, this effect is small as line width caused by the electron impact broadening is comparable or even larger than that of AI resonance broadening.

After investigating the effect of AI resonance broadening on the opacity of Ge plasma, we turn to the comparison of our theoretical results with the experimental data. **Figure 5** shows the calculated transmission of Ge plasma at temperatures of 58, 60 and 62 eV, while the mass density is fixed to be  $0.01 \text{ g/cm}^3$  in solid lines. The dashed lines show the experimental data measured by Renaudin *et al.* [3]. Areal density used in the calculations is equal to  $0.11 \text{ mg/cm}^2$ . It can be seen that the transmission is sensitive to the temperature of the plasmas, in particular in 2p-3d region. At the temperature of 58 eV, there is a close agreement for absorption line position between theory and experiment at the higher photon energy wing of the 2p-3d (1300 - 1340 eV), while such a good agreement turned to the lower photon energy region (1220 - 1260 eV) at the temperature of 62 eV. This shows that there is small temperature or density gradient in the experiment. In the whole shown photon energy range,

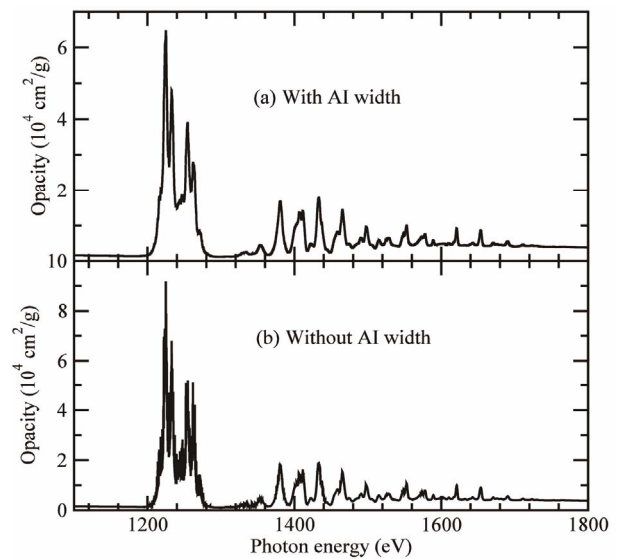


**Figure 4.** The effect of AI resonance broadening on the radiative opacity of Ge plasma at a temperature of 38 eV and a density of  $0.015 \text{ g/cm}^3$ : (a) including and (b) not including such an effect.

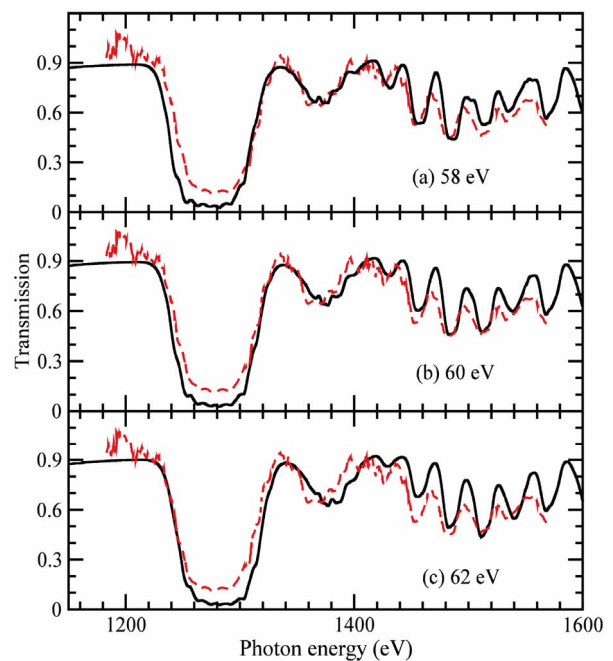


**Figure 5.** Transmission of Ge plasma at temperatures of (a) 58; (b) 60 and (c) 62 eV with the mass density being  $0.01 \text{ g/cm}^3$  in solid lines. The dashed lines refer to the experimental data of Renaudin *et al.* [3].

there is a better agreement between theory and experiment at the temperature of 60 eV, which is consistent with the experimental determination of plasma temperature from element tracer of Mg and radiative-hydrodynamic simulations [3]. At the temperature of 60 eV, a more complete comparison between experiment and dif-

ferent theoretical results is shown in **Figure 6**. Two additional theoretical results are compared in **Figure 6** which were obtained by average atom calculations including UTA with and without orbital relaxation (OR) treatment [3]. Renaudin *et al.* [3] also carried out DLA calculations, yet it is difficult to extract the data from the original figure.

At the experimental condition of Renaudin *et al.* [3], the 2p-3d absorption does not show an interval of spin-orbit splitting.  $2p_{3/2} - 3d_{5/2}$  and  $2p_{1/2} - 3d_{3/2}$  are smoothly merged together, expanding an extended photon energy region from 1220 to 1320 eV. Similar conclusion applies for the experimental spectra of Foster *et al.* [1]. To save space, we do not show detailed comparison between theory and experiment under the physical condition of Foster *et al.* [1]. With the decrease of plasma temperature, the separation of 2p-3d spin-orbit splitting begins to appear evidently. Such a trend can easily be seen from **Figures 7** and **8**, which shows the transmission at temperatures near 38 eV and 24 eV.

In **Figure 7**, the spectrally resolved transmission of Ge plasma are shown in solid lines at temperatures of 36, 38 and 40 eV with the mass density being fixed to be  $0.012 \text{ g/cm}^3$ . The dashed lines shows the experimental data measured by Perry *et al.* [2] with the temperature being determined to be  $38 \pm 2 \text{ eV}$  and density  $0.012 \pm 0.003 \text{ g/cm}^3$ . In plot (b), the STA prediction is also given for Ge plasma at the temperature of 38 eV. Areal density used in the calculations is equal to  $0.111 \text{ mg/cm}^2$ . In this case, the 2p-3d spin-orbital splitting is very sensitive to the temperature of the plasmas. With just 2 eV difference in temperature from (a) to (c), the 2p-3d spin-orbital

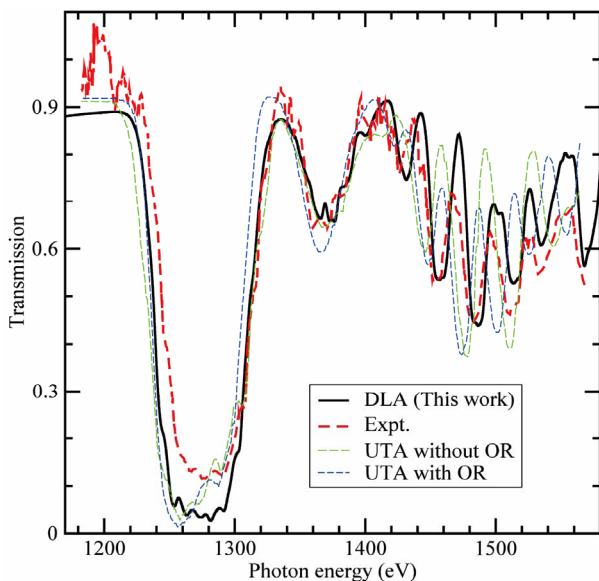


**Figure 6.** Comparison of different theoretical (DLA and UTA) and experimental spectra of transmission of Ge plasma at a temperature of 60 eV and a density of 0.01.

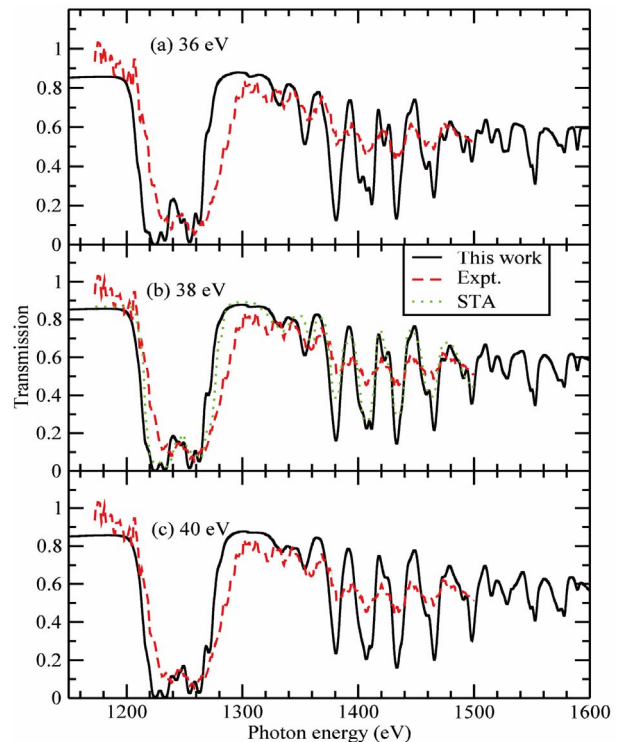


**Figure 7.** Transmission of Ge plasma at temperatures of (a) 36; (b) 38 and (c) 40 eV with the mass density being  $0.012 \text{ g/cm}^3$  in solid lines. The dashed lines refer to the experimental data of Perry *et al.* [2].

splitting is much more obvious at 36 eV than at 40 eV, even the shape of absorption structures is much different at the three temperatures. For example, look at the absorption feature near photon energy 1240 eV. The absorption structure for the spin-orbital splitting is sharper at 36 eV than at 38 and 40 eV. For the wide and relatively flat absorption bottom at 38 and 40 eV, the variation trend with photon energy is reversed. This is an indication that the 2p-3d absorption has the potential of temperature diagnosis, especially in temperature region where absorption is very sensitive to the temperature. As there are enormous numbers of absorption lines, the individual lines merged to become quasi-continuum absorption bands, DLA results tend to agree with UTA and STA ones. Note, however, that at some particular temperature, where there are not so many absorption lines to merge together, DLA results will have distinct difference from those of UTA and STA.

The 2p-3d spin-orbit splitting becomes more evident with the further decrease of temperature. In **Figure 8**, the spectrally resolved transmission of Ge plasma are shown in solid lines at temperatures of 16, 18, 20, 22 and 24 eV and the mass density being fixed to be  $0.015 \text{ g/cm}^3$ . The dashed lines shows the experimental data [4,11]. In plot (e), the SCO and SCORCG predictions [11,27] are given for Ge plasma at temperature of 24 eV. Areal density

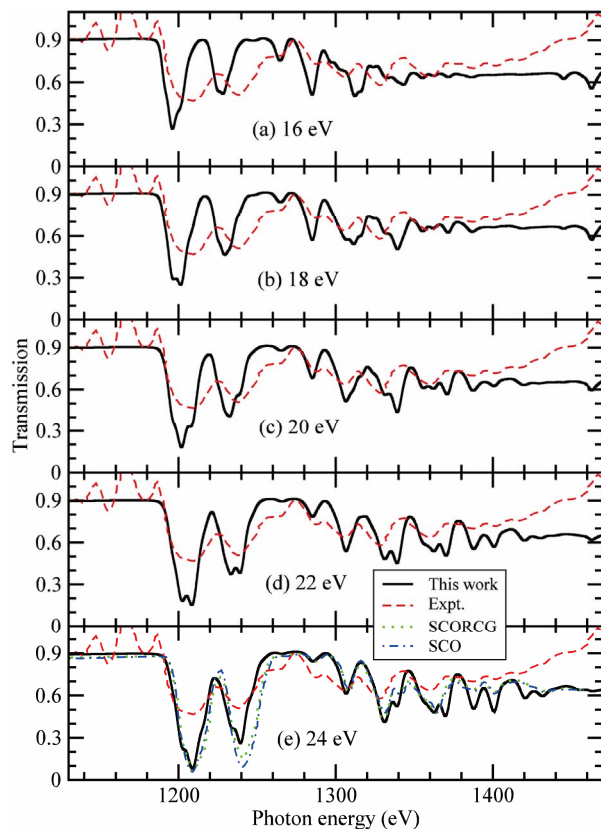


**Figure 8.** Transmission of Ge plasma at temperatures of (a) 16; (b) 18; (c) 20; (d) 22 and (e) 24 eV with the mass density being  $0.015 \text{ g/cm}^3$  in solid lines. The dashed lines refer to the experimental data [11,13]. In plot (f), the dotted and dot-dashed lines refer to results of SCO and SCORCG codes, respectively.

used in the calculations is equal to  $0.08 \text{ mg/cm}^2$ . At these temperatures, the shape and intensity of the 2p-3d spin-orbital splitting is more sensitive to the temperature of the plasmas than in physical conditions of **Figures 5** and **7**. With just 2 eV difference in the temperature, the shape and relative intensity of the 2p-3d spin-orbital splitting is noticeably different from case to case for plot (a)-(e), and therefore the potential of temperature diagnosis at these temperatures is better than in **Figures 5** and **7**. Reasonable agreement is found between our work and those of SCO and SCORCG predictions at 24 eV, although stronger absorption is predicted by SCO and SCORCG codes for the  $2p_{1/2} - 3d_{3/2}$  transition lines near the photon energy 1240 eV. Compared with the experiment, all theoretical results deviate from experimental spectrum, in particular in the 2p-3d region of 1190 - 1260 eV. Such a deviation is due to the strong gradients of temperature and density in the experimental plasma.

In conclusion, spectrally resolved L-shell absorption spectra of open-M-shell germanium plasmas were investigated by using a detailed line-by-line method. In the

DLA approach, spectral line profile plays an important role on the radiative opacity of plasmas. In this work, we focus on the effect of AI resonance broadening on the L-shell absorption of germanium plasmas. It was found that for plasmas at typical present and past experimental conditions, line width due to AI resonance broadening is an order of magnitude larger than that due to electron impact and Doppler broadenings. For germanium ion with near closed atomic structure such as  $\text{Ge}^{14+}$ , the effect of AI resonance broadening is most pronounced with the peak absorption cross section of one particular 2p-3d absorption line being an order of magnitude smaller than that of not including this effect. For germanium ion with near half filled 3d or 3p electron such as  $\text{Ge}^{9+}$  and  $\text{Ge}^{16+}$ , such an effect is not so pronounced due to many 2p-nd transition lines merged together to form quasi-continuum bands. Detailed comparisons are carried out with available experimental spectra at different physical conditions of different plasma temperatures and densities. The results show that absorption spectra are sensitive to the temperature of plasmas and show the potential of temperature diagnostics by using the 2p-3d transition arrays. The relative shape and intensity of the 2p-3d spin-orbit splitting is very sensitive to the temperature and therefore should be an ideal tool of temperature diagnostics.

#### 4. Acknowledgements

This work was supported by the National Natural Science Foundation of China under Grant Nos. 11274382, 11274383, and 11204376.

#### REFERENCES

- [1] J. M. Foster, D. J. Hoarty, C. C. Smith, P. A. Rosen, S. J. Davidson, S. J. Rose, T. S. Perry and F. J. D. Serduke, "L-Shell Absorption Spectrum of an Open-M-Shell Germanium Plasma: Comparison of Experimental Data with a Detailed Configuration-Accounting Calculation," *Physical Review Letter*, Vol. 67, No. 23, 1991, pp. 3255-3258. [doi:10.1103/PhysRevLett.67.3255](https://doi.org/10.1103/PhysRevLett.67.3255)
- [2] T. S. Perry, K. S. Budil, R. Cauble, R. A. Ward, D. R. Back, C. A. Iglesias, B. G. Wilson, J. K. Nash, C. C. Smith, J. M. Foster, S. J. Davidson, F. J. D. Serduke, J. D. Kilkenny and R. W. Lee, "Quantitative Measurement of Mid-z Opacities," *Journal of Quantitative Spectroscopy & Radiative Transfer*, Vol. 54, No. 1-2, 1995, pp. 317-324. [doi:10.1016/0022-4073\(95\)00066-T](https://doi.org/10.1016/0022-4073(95)00066-T)
- [3] P. Renaudin, C. Blancard, J. Bruneau, G. Faussurier, J.-E. Fuchs and S. Gary, "Absorption Experiments on X-Ray-Heated Magnesium and Germanium Constrained Samples," *Journal of Quantitative Spectroscopy & Radiative Transfer*, Vol. 99, No. 1-3, 2006, pp. 511-522. [doi:10.1016/j.jqsrt.2005.05.041](https://doi.org/10.1016/j.jqsrt.2005.05.041)
- [4] G. Loisel, P. Arnault, S. Bastiani-Ceccotti, T. Blenski, T.

- Caillaud, J. Fariaut, W. Folsner, F. Gilleron, J.-C. Pain, M. Poirier, C. Reverdin, V. Silvert, F. Thais, S. Turck-Chieze and B. Villette, "Absorption Spectroscopy of Mid and Neighboring Z Plasmas: Iron, Nickel, Copper and Germanium," *High Energy Density Physics*, Vol. 5, No. 3, 2009, pp. 173-181. [doi:10.1016/j.hedp.2009.05.015](https://doi.org/10.1016/j.hedp.2009.05.015)
- [5] D. J. Hoarty, S. F. James, C. R. D. Brown, B. M. Williams, H. K. Chung, J. W. O. Harris, L. M. Upcraft, B. J. B. Crowley, C. C. Smith and R. W. Lee, "Measurements of Emission Spectra from Hot, Dense Germanium Plasma in Short Pulse Laser Experiments," *High Energy Density Physics*, Vol. 6, No. 1, 2010, pp. 105-108. [doi:10.1016/j.hedp.2009.05.019](https://doi.org/10.1016/j.hedp.2009.05.019)
- [6] J. W. O. Harris, L. M. Upcraft, D. J. Hoarty, B. J. B. Crowley, C. R. D. Brown and S. F. James, "A Comparison of Theory and Experiment for High Density, High Temperature Germanium Spectra," *High Energy Density Physics*, Vol. 6, No. 1, 2010, pp. 95-98. [doi:10.1016/j.hedp.2009.06.001](https://doi.org/10.1016/j.hedp.2009.06.001)
- [7] Y. L. Peng, D. Xia and J. M. Li, "A Generalized Quasi-Sum Relations for Oscillator Strengths in Transition Arrays: Theoretical Study of the Opacity of Ge Plasmas," *Journal of Quantitative Spectroscopy & Radiative Transfer*, Vol. 87, No. 1, 2004, pp. 95-106. [doi:10.1016/j.jqsrt.2003.12.024](https://doi.org/10.1016/j.jqsrt.2003.12.024)
- [8] V. J. L. White, J. M. Foster, J. C. V. Hansom and P. A. Rosen, "Measurements of Radiation Heat Transport in Germanium: Validation of a Break of an Opacity Model," *Physical Review E*, Vol. 49, No. 6, 1994, pp. R4803-R4806. [doi:10.1103/PhysRevE.49.R4803](https://doi.org/10.1103/PhysRevE.49.R4803)
- [9] J. Yan and J. M. Li, "Theoretical Simulation of the Transmission Spectra of Fe and Ge Plasmas," *Chinese Physical Letter*, Vol. 17, No. 3, 2000, pp. 194-196. [doi:10.1088/0256-307X/17/3/014](https://doi.org/10.1088/0256-307X/17/3/014)
- [10] A. Bar-Shalom, J. Oreg and W. H. Goldstein, "Configuration Interaction in LTE Spectra of Heavy Elements," *Journal of Quantitative Spectroscopy & Radiative Transfer*, Vol. 51, No. 1-2, 1994, pp. 27-39. [doi:10.1016/0022-4073\(94\)90062-0](https://doi.org/10.1016/0022-4073(94)90062-0)
- [11] T. Blenski, G. Loisel, M. Poirier, F. Thais, P. Arnault, T. Caillaud, J. Fariaut, F. Gilleron, J.-C. Pain, Q. Porcherot, C. Reverdin, V. Silvert, B. Villette, S. Bastiani-Ceccotti, S. Turck-Chieze, W. Folsner and F. de Gaufridy De Dortan, "Theoretical Interpretation of X-Rays Photo-Absorption in Medium-Z Elements Plasmas Measured at LULI-2000 Facility," *High Energy Density Physics*, Vol. 7, 2011, pp. 320-326. [doi:10.1016/j.hedp.2011.06.004](https://doi.org/10.1016/j.hedp.2011.06.004)
- [12] Q. Porcherot, J. C. Pain, F. Gilleron and T. Blenski, "A Consistent Approach for Mixed Detailed and Statistical Calculation of Opacities in Hot Plasmas," *High Energy Density Physics*, Vol. 7, No. 4, 2011, pp. 234-239. [doi:10.1016/j.hedp.2011.05.001](https://doi.org/10.1016/j.hedp.2011.05.001)
- [13] F. Gilleron, J. C. Pain, Q. Porcherot, J. Bauche and C. Bauche-Arnault, "Corrections to Statistical Modeling of Spectra for Plasmas at Moderate or Low Temperatures," *High Energy Density Physics*, Vol. 7, No. 4, 2011, pp. 277-284. [doi:10.1016/j.hedp.2011.05.005](https://doi.org/10.1016/j.hedp.2011.05.005)
- [14] J. A. Gaffney and S. J. Rose, "The Effect of Unresolved Transition Arrays on Plasma Opacity Calculations," *High Energy Density Physics*, Vol. 7, No. 4, 2011, pp. 240-246. [doi:10.1016/j.hedp.2011.05.003](https://doi.org/10.1016/j.hedp.2011.05.003)
- [15] C. J. Fontes, J. Abdallah Jr., C. Bowen, R. W. Lee and Yu Ralchenko, "Review of the NLTE-5 Kinetics Workshop," *High Energy Density Physics*, Vol. 5, No. 1-2, 2009, pp. 15-22. [doi:10.1016/j.hedp.2009.02.004](https://doi.org/10.1016/j.hedp.2009.02.004)
- [16] J. R. Albritton and B. G. Wilson, "Non-LTE Ionization and Energy Balance in High-Z Laser Plasmas Including Two-Electron Transitions," *Physical Review Letter*, Vol. 83, No. 8, 1999, pp. 1594-1597. [doi:10.1103/PhysRevLett.83.1594](https://doi.org/10.1103/PhysRevLett.83.1594)
- [17] Y. Hahn, "Electron-Ion Recombination Processes: An Overview," *Reports on Progress in Physics*, Vol. 60, No. 7, 1997, pp. 691-759. [doi:10.1088/0034-4885/60/7/001](https://doi.org/10.1088/0034-4885/60/7/001)
- [18] V. L. Jacobs, "Autoionization Phenomena in Plasma Radiation Processes," *Journal of Quantitative Spectroscopy & Radiative Transfer*, Vol. 54, No. 1-2, 1995, pp. 195-205. [doi:10.1016/0022-4073\(95\)00055-P](https://doi.org/10.1016/0022-4073(95)00055-P)
- [19] J. Bauche, C. Bauche-Arnault and O. Peyrusse, "Role of Dielectronic Recombination and Autoionizing States in the Dynamic Equilibrium of Non-LTE Plasmas," *High Energy Density Physics*, Vol. 5, No. 1-2, 2009, pp. 51-60. [doi:10.1016/j.hedp.2009.02.003](https://doi.org/10.1016/j.hedp.2009.02.003)
- [20] V. L. Jacobs, "Kinetic and Spectral Descriptions for Atomic Processes Involving Autoionizing Resonances in High-Temperature Plasmas," *High Energy Density Physics*, Vol. 5, No. 1-2, 2009, pp. 80-88. [doi:10.1016/j.hedp.2009.03.001](https://doi.org/10.1016/j.hedp.2009.03.001)
- [21] C. Gao and J. L. Zeng, "Validity of Analytical Formulas for Autoionization and Dielectronic Capture Rates Used in Collisional-Radiative Models," *Physical Review A*, Vol. 82, No. 6, 2010, pp. 1-8. [doi:10.1103/PhysRevA.82.062515](https://doi.org/10.1103/PhysRevA.82.062515)
- [22] R. D. Cowan, "The Theory of Atomic Structure and Spectra," University of California Press, Berkeley, 1981.
- [23] M. S. Dimitrijevic and N. Konjevic, "Stark Widths of Doubly- and Triply-Ionized Atom Lines," *Journal of Quantitative Spectroscopy & Radiative Transfer*, Vol. 24, No. 6, 1980, pp. 451-459. [doi:10.1016/0022-4073\(80\)90014-X](https://doi.org/10.1016/0022-4073(80)90014-X)
- [24] M. S. Dimitrijevic and N. Konjevic, "Simple Estimates for Stark Broadening of Ion Lines in Stellar Plasmas," *Astronomy & Astrophysics*, Vol. 172, 1987, pp. 345-349.
- [25] D. J. Heading, J. S. Wark, G. R. Bennett and R. W. Lee, "Simulations of Spectra from Dense Aluminium Plasmas," *Journal of Quantitative Spectroscopy & Radiative Transfer*, Vol. 54, No. 1-2, 1995, pp. 167-180.
- [26] M. F. Gu, "Indirect X-Ray Line-Formation Process in Iron L-Shell Ions," *The Astrophysical Journal*, Vol. 582, No. 2, 2003, pp. 1241-1250. [doi:10.1086/344745](https://doi.org/10.1086/344745)
- [27] F. Gilleron, J. Bauche and C. Bauche-Arnault, "A Statistical Approach for Simulating Detailed-Line Spectra," *Journal of Physics B: Atomic, Molecular and Optical Physics*, Vol. 40, No. 15, 2007, pp. 3057-3074. [doi:10.1088/0953-4075/40/15/007](https://doi.org/10.1088/0953-4075/40/15/007)